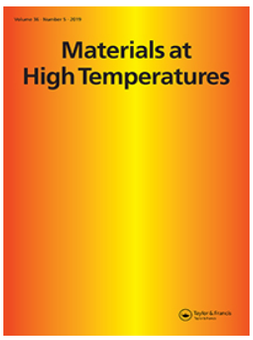

Materials at High Temperatures

ISSN: 0960-3409 (Print) 1878-6413 (Online) Journal homepage: https://www.tandfonline.com/loi/ymht20

Procedures for handling computationally heavy cyclic load cases with application to a disc alloy material

Daniel Leidermark & Kjell Simonsson

To cite this article: Daniel Leidermark & Kjell Simonsson (2019) Procedures for handling computationally heavy cyclic load cases with application to a disc alloy material, Materials at High Temperatures, 36:5, 447-458, DOI: 10.1080/09603409.2019.1631587

To link to this article: https://doi.org/10.1080/09603409.2019.1631587

© 2019 The Author(s). Published by Informa UK Limited, trading as Taylor & Francis Group.

Published online: 20 Jun 2019.

Submit your article to this journal

Article views: 601

View related articles

View Crossmark data

Citing articles: 3 View citing articles

Full Terms & Conditions of access and use can be found at
https://www.tandfonline.com/action/journalInformation?journalCode=ymht20

MATERIALS AT HIGH TEMPERATURES
2019, VOL. 36, NO. 5, 447–458
https://doi.org/10.1080/09603409.2019.1631587

Taylor & Francis
Taylor & Francis Group

OPEN ACCESS Check for updates

Procedures for handling computationally heavy cyclic load cases with application to a disc alloy material

Daniel Leidermark and Kjell Simonsson

Division of Solid Mechanics, Linköping University, Linköping, Sweden

ABSTRACT

The computational efficiency in analysing cyclically loaded structures is a highly prioritised issue for the gas turbine industry, as a cycle-by-cycle simulation of *e.g.* a turbine disc is far too time consuming. Hence, in this paper, the efficiency of two different procedures to handle computational expansive load cases, a numerical extrapolation and a parameter modification procedure, are evaluated and compared to a cycle-by-cycle simulation. For this, a local implementation approach was adopted, where a user-defined material subroutine is used for the cycle jumping procedures with good results. This in contrast to a global approach where the finite element simulation is restarted and mapping of the solution is performed at each cycle jump. From the comparison, it can be observed that the discrete parameter modification procedure is by margin the fastest one, but the accuracy depends on the material parameter optimisation routine. The extrapolation procedure can incorporate stability and/or termination criteria.

ARTICLE HISTORY
Received 11 April 2018
Accepted 3 June 2019

KEYWORDS
Cycle jumping; cyclic response; computational efficiency; gas turbine disc alloy; user-defined material subroutine

Introduction

Gas turbines (both for propulsion and power generation) will by necessity continue to play a central role in order to reach a more sustainable energy and resource usage system for the future. There is a strong need for making these machines more efficient than today, which calls for higher combustion temperatures. Furthermore, with the increasing amount of renewable energy sources, which are inherently intermittent, the running profile of stationary power generating machines has to change to more cyclic operation, as they will be used for balancing the grid. In this context, more efficient cooling, material characterisation and life assessment models are of importance.

In order to accurately predict the life of components subjected to isothermal or thermomechanical fatigue loading situations, it is of importance to correctly predict the local stress-strain history. A fatigue life evaluation process can in principle be performed using finite element (FE) analysis to simulate every load cycle with respect to time until failure. However, even with the computational power of today, a complete cycle-by-cycle analysis is generally far too time-consuming, with regard to the often complex geometry of the component, material behaviour and thousands of load cycles, and thus, a cycle jumping scheme needs to be invoked.

The usage of a cycle jumping procedure will speed-up the computational evaluation in an FE-analysis, where a couple of cycles are evaluated and the material state is updated (cycle jump) with respect to a large number of cycles. Thus, from a computational point of view, the gain lies in the number of cycles that need to be carried out. The success of such a procedure relies on the fact that even if the different fields may momentarily vary rapidly or in-homogeneously within each cycle (or sequence), their values at a specific instant/point of the cycle vary slowly with respect to the cycle number. However, it is important that an accurate prediction is maintained. There is a vast entity of published work in the field of cycle jumping procedures, each refining the implementation, adding new unique features or just using the tool as a 'black-box' for speeding-up their computations. Different areas are touched, as well as materials, but a common denominator is cyclic loadings. For further details regarding cycle jumping and relevant application areas, see *e.g.* [1–9].

The most direct way to accomplish a cycle jumping scheme is to base it on a Taylor expansion, where a chosen number of full/complete load cycle simulations at cycle N provide the basis for the prediction of the state at cycle $N + \Delta N$. Furthermore, by evaluating the influence of additional full cycle simulations at cycle N, see *e.g.* [10–13], or by evaluating some full cycles at cycle $N + \Delta N$, see *e.g.* [14,15], a posteriori error estimation can be obtained for the step $N \rightarrow N + \Delta N$. Thus, in an adaptive context, an unsuccessful step may then be redone with a smaller ΔN and/or higher degree of approximation (based on

CONTACT Daniel Leidermark daniel.leidermark@liu.se

© 2019 The Author(s). Published by Informa UK Limited, trading as Taylor & Francis Group.
This is an Open Access article distributed under the terms of the Creative Commons Attribution-NonCommercial-NoDerivatives License (http://creativecommons.org/licenses/by-nc-nd/4.0/), which permits non-commercial re-use, distribution, and reproduction in any medium, provided the original work is properly cited, and is not altered, transformed, or built upon in any way.

more full cycle simulations at cycle N). A different numerical approach than the Taylor extrapolation scheme exists in Abaqus [16], the direct cyclic algorithm. This method allows for a direct way to obtain the stabilised state, based on a modified Newton method in conjunction with Fourier series of the solution and the residual.

An alternative approach for reducing the computational effort is to artificially change the material parameters, such that the stress-strain history can be obtained by a substantially reduced number of full cycle simulations. This may be done by a 'continuous' cycle scaling approach, see *e.g.* Brommesson *et al.* [17], where the constitutive parameters are optimised to accommodate the reduced number of cycles, or by a 'point wise/discrete' approach, where the constitutive parameters are optimised to reflect the behaviour at selected instances, typically only midlife, see *e.g.* Hasselqvist [18]. In the first approach, a normal type of elasto-plastic analysis is performed for a reduced number of load cycles but with modified material parameters, while in the second case a couple of initial cycles are carried out with virgin material data, followed by a change of material parameters (midlife), and a couple of new load cycles with the new data (a procedure which can directly be generalisable to more discrete points). The most obvious benefit of the latter discrete approach is that a much simpler constitutive description may be adopted, as *e.g.* cyclic hardening/softening or ageing does not need an evolution description.

Even though cycle jumping is not a new issue in the literature, focus has mainly been placed on the Taylor expansion paradigm. Furthermore, hardly any work has focused on comparing the two basic approaches, and their relative pros and cons, which is the aim of the present work. More specifically, the present study investigates how well the discrete material parameter modification approach captures the cyclic behaviour of a simple component with a stress raiser under strain-controlled cyclic loading, and which speed-ups that can be achieved with respect to a basic extrapolation (Taylor approximation) approach (without error control/adaptivity) in an FE-context. The geometry has deliberately been chosen as simple as possible in order not to let a complex geometry obscure (influence) the analysis and comparison, but still encompassing the type of inhomogeneous fields of stress and strain found at local stress raisers in gas turbine components. Material properties and observed cyclic behaviour for a common disc alloy material, taken from the literature, was used in the evaluation.

Constitutive model

As mentioned previously, components in a gas turbine are exposed to severe loading conditions, due to the cyclic nature of loading arising from *e.g.* the repeated starts and stops for a stationary gas turbine balancing the power grid or the many take-offs and landings for an aircraft engine operating midrange distances. Under these circumstances a component such as a turbine disc will experience thermomechanical fatigue [19–21], low-cycle fatigue [22–24], high-cycle fatigue [25], creep [26], mean stress relaxation [27], creep-fatigue crack growth [28], dwell crack growth [29] *etc.*, and thus, an appropriate constitutive model needs to be utilised to account for the behaviour of the material. Focusing attention on disc alloys, as a non-linear hardening behaviour is generally adopted, see *e.g.* [24,30–34]. The constitutive model adopted in this work is based on the non-linear kinematic hardening law proposed by Ohno and Wang [35,36] in conjunction with a saturated isotropic hardening law, *cf.* Chaboche [37]. In what follows, all tensors are presented in index notation, where second-order tensors are quantified by upper-case Roman or Greek-letters and scalar-valued parameters are defined by lower-case Roman and Greek-letters. The following yield function is employed

$$f = \sigma_{eq}^{vM}\left[\hat{\sigma}_{ij} - B_{ij}\right] - r - \sigma_Y \tag{1}$$

where $\hat{\sigma}_{ij}$ represents the deviatoric stress tensor and B_{ij} is the back-stress tensor. The drag-stress (isotropic hardening) is described by r, σ_Y is the initial yield limit and σ_{eq}^{vM} is the von Mises equivalent stress, defined as

$$\sigma_{eq}^{vM} = \sqrt{\frac{3}{2}\left(\hat{\sigma}_{ij} - B_{ij}\right)\left(\hat{\sigma}_{ij} - B_{ij}\right)} \tag{2}$$

The evolution law of the plastic strain tensor is defined by the flow rule based on the adopted yield function as

$$\dot{\varepsilon}_{ij}^{p} = \dot{\lambda}\frac{\partial f}{\partial \sigma_{ij}} = \dot{\lambda}\frac{3}{2}\frac{\hat{\sigma}_{ij} - B_{ij}}{\sigma_{eq}^{vM}} \tag{3}$$

where $\dot{\lambda}$ is the plastic multiplier. Furthermore, it can also be observed that no viscous effects are included in the study, as the aim is to analyse and compare cycle jumping procedures.

Based on Chaboche [38], the total back-stress may be additively decomposed by several back-stress terms $B_{ij} = \sum_{k=1}^{N_B} B_{ij}^{k}$ to increase the accuracy, where the following evolution law for each individual term in this work is taken to be given by

$$\dot{B}_{ij}^{k} = \frac{2}{3}c_k\dot{\varepsilon}_{ij}^{p} - \gamma_k\left(\frac{b_k}{w_k}\right)^{m_k}\left\langle\frac{\dot{\varepsilon}_{pq}^{p}B_{pq}^{k}}{b_k}\right\rangle B_{ij}^{k} \tag{4}$$

with the definition $b_k = \sqrt{\frac{3}{2}B_{ij}^{k}B_{ij}^{k}}$. The material parameters c_k and γ_k govern the linear and the recovery term, respectively, $\langle\bullet\rangle$ is the Macaulay bracket and finally the value of m_k controls the ratcheting or mean stress relaxation rate due to the non-linearity

of the power function. For $m_k \to \infty$ the model yields no ratcheting or mean stress relaxation when b_k is below the critical state $w_k = c_k/\gamma_k$, thus reverting back to a pure linear hardening model. With decreasing values an increasing ratcheting or mean stress relaxation is obtained.

An additive decomposition is also employed for the total drag-stress, $r = \sum_{k=1}^{N_r} r_k$, to correlate to the different stages of the cyclic evolution behaviour. Hence, the evolution law of the saturated isotropic hardening law from Chaboche [37] for each individual term is given by

$$\dot{r}_k = a_k(q_k - r_k)\dot{\lambda} \tag{5}$$

in which the material parameter a_k describes the rate of cyclic hardening/softening and where the saturation is directly included in the model by the material parameter q_k.

The above presented constitutive model has been implemented as a user-defined material subroutine in FORTRAN, to be used in an FE-context. It was based on the incremental total strain tensor ($\Delta\varepsilon_{ij}^{tot}$) as input, and subsequently, only the back-stress and drag-stress components need to be stored as history variables and reused at the beginning of the next time-step.

Material parameters

As no experiments have been performed within this study, the material parameters were quantified based on available literature data of an appropriate disc alloy. Gustafsson *et al.* [32] performed isothermal cyclic experiments on the disc alloy IN718 at 400°C and specified material parameters for an Ohno-Wang model with three back-stress terms, which was coupled with three linear isotropic hardening terms. The use of three back-stress terms ($N_B = 3$) in the constitutive model and values for the back-stress parameters, Young's modulus, Poisson's ratio and initial yield limit were adopted from that work. As a different isotropic hardening evolution law was adopted in this work, a new set of parameters needed to be defined. Hence, the values of the drag-stress parameters, using three terms ($N_r = 3$), were obtained by an optimisation of the maximum and minimum stress data from the experiments in Gustafsson *et al.* [32] using the built-in *lsqnonlin* function in MATLAB [39]. Based on the three back-stress and drag-stress terms in this work, a satisfactory prediction of the material response with respect to the experimental hysteresis loop and cyclic softening, *cf.* [32], was obtained. The material parameters can be found in Table 1. It is to be noticed that even though the loading and material in this work have been chosen to represent turbine disc applications the adopted cycle jumping procedures do have a general applicability to other materials and applications.

Table 1. Material parameters for the constitutive model.

Parameter	Value	Units
σ_Y	864.20	MPa
E	187	GPa
ν	0.32	–
c_1	370.23	GPa
c_2	147.01	GPa
c_3	34.36	GPa
γ_1	4776.87	–
γ_2	987.20	–
γ_3	171.52	–
m_1	12	–
m_2	12	–
m_3	12	–
a_1	1622.78	–
a_2	1229.46	–
a_3	2.607	–
q_1	− 99.04	MPa
q_2	− 35.007	MPa
q_3	− 65.609	MPa

Evaluated cycle jumping procedures

As advertised earlier, the numerical extrapolation method and the discrete material parameter modification method will be evaluated and compared. The two approaches and implementation aspects are presented in detail below.

Implementation framework

Independently of the type of applied cycle jumping scheme, different implementation frameworks can be adopted. One way is to define/implement a global framework surrounding the FE-analysis, which explicitly extracts internal state variables and global responses after each finished time step to extrapolate these forward. This can be done by saving the extracted variables in an external database to handle the large quantity of previous and updated variables, mapping these onto the FE-model to get the corresponding internal state variables and global responses (*e.g.* stress state, displacements, contact conditions …) for the updated state, and restarting the FE-analysis. Another way, which has been implemented and used in this study, is a so called local implementation approach. Here, the available user-defined material subroutine enables a direct control of the adopted cycle jumping procedure. As the cycle jumping procedure can be directly implemented into the user-defined subroutine as an add-on, in close connection to the material model, the history variables keep track of the previous cycles state to be used in the cycle jump. Hence, everything is handled on the local level in the user-defined material subroutine with respect to the element. This local approach of implementation

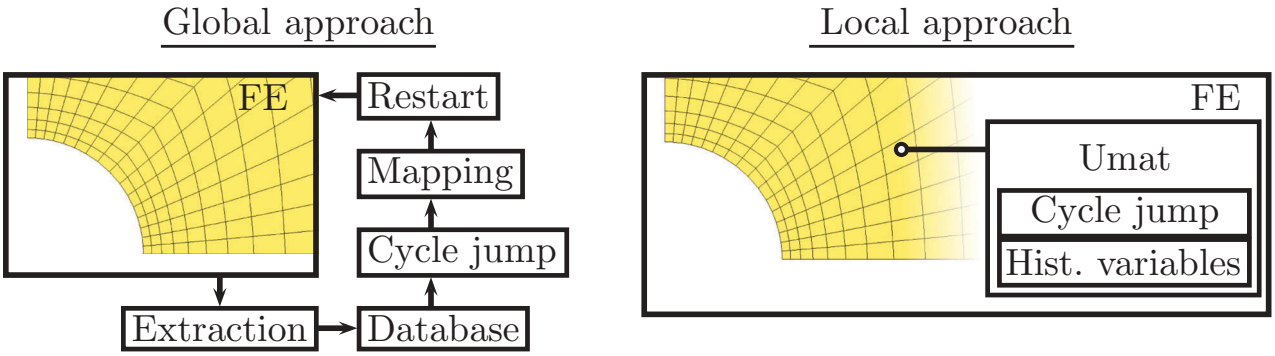

Figure 1. Local and global implementation approaches for the cycle jumping procedures.

gives a more straightforward application of the cycle jumping procedure compared to a global implementation approach, see Figure 1. On the downside, only static or discrete stepping of ΔN can be used in the local approach for the numerical extrapolation cycle jumping scheme (described below) for FE-models consisting of multiple elements/integration points, as the user-defined material subroutine is applied per integration point and the variables in the response set are related to that specific integration point. Hence, an adaptive (dynamic) approach which is able to either increase or decrease ΔN based on *e.g.* the stress state would incline that different extrapolation step sizes are generated locally within the FE-model, and such a dynamic method is thus not applicable locally (per integration point). This can be handled by a global approach as all responses will be available and any kind of control measure (adaptive ΔN, accuracy and/or termination control) can be adopted due to the global state. An alternative possible approach for the local implementation can be to define a certain cycle jump size for all elements in the beginning of the initial softening and later switch to another size when the rapid initial softening has diminished. This can, of course, be done continuously over the elapsed time of the simulation, by discretely increasing the jumping size with a number of performed cycles at distinct times.

Extrapolation method

The first approach is the numerical extrapolation method, where the common denominator is the use of a Taylor expansion of the internal state variables and global responses. The response set $\mathcal{F}_N$ obtained in the FE-simulation at cycle N, containing internal state variables and global responses, are extrapolated ΔN cycles forward, according to the standard Taylor expansion

$$\mathcal{F}_{N+\Delta N} = \sum_{n=0}^{m} \frac{1}{n!} \frac{\partial^{(n)} \mathcal{F}_N}{\partial N^{(n)}} \Delta N^n \tag{6}$$

Based on this type of extrapolation, Lin *et al.* [10] evaluated components undergoing cyclic thermal loading combined with constant mechanical loading. They defined a number of criteria when the cycle jumping was to initiate and terminate, based on the steady-state condition as well as acceptable stress change, rate of ratcheting and change in damage. A further study was performed by Johansson and Ekh [11], focusing on the accuracy of the solution, where they adopted an adaptive extrapolation procedure with respect to the received error. An extrapolation procedure based on linear shape functions was presented by Wang *et al.* [14], where the use of linear shape functions was motivated by the stability of these compared to polynomial functions, which are more accurate but very sensitive to the size of extrapolation step and in need of more supporting points. To account for erroneous results in the new extrapolated state, a backward extrapolation was used to control the accuracy by a set of conventional cycles from the extrapolated state and the relative error was compared to a defined limit. The above implementation was further enhanced by Kontermann *et al.* [15], by introducing a multi-parallel processing capability.

In the present study the above described local implementation approach has been used, where an updated user-defined material subroutine also includes subroutines which saves the variable values for each cycle, reads these saved variables and extrapolates the variables. The procedure is based on a first-order Taylor expansion, setting $m = 1$ in Equation (6), hence

$$\mathcal{F}_{N+\Delta N} = \mathcal{F}_N + \frac{\mathrm{d}\mathcal{F}_N}{\mathrm{d}N} \Delta N = \mathcal{F}_N + \frac{\mathcal{F}_N - \mathcal{F}_{N-1}}{1} \Delta N \tag{7}$$

where $\mathrm{d}N = 1$ is due to that only one cycle separates the two time-frames of the saved variables, and in this case, the response set contains the stress tensor, the three individual back-stress tensors and the three

drag-stresses, hence $\mathcal{F} = \mathcal{F}\left[\sigma_{ij}, B_{ij}^{k}, r_{k}\right]$. These seven fields are the only variables that locally vary over the time-step and need to be extrapolated, other variables are generated within the iterative process of the user-defined material subroutine.

The observed response from the cyclic experiments displays a smooth softening (mean stress relaxation) behaviour, beginning with a steep descent that stabilises with an increased number of cycles, see Gustafsson *et al.* [32]. Based on this, the first four extrapolation steps are performed with a ΔN equal to 2 and onward followed by 10. This is due to stability reasons with the steep descent, as a 'too' large step might generate an unstable response. Note that the aim of this paper is not to evaluate the continuous accuracy or to develop an innovative extrapolation procedure; hence, no consideration has been spent on these matters. Instead, focus is on simplicity and comparison of the two basic approaches.

Parameter modification method

The second approach, the discrete material parameter modification method, is fast and straightforward. In this method, no extrapolation is performed, and by this, no stability or accuracy controls can or need to be utilised. Furthermore, it is an appropriate procedure to use from a post-processing fatigue life evaluation point of view, as only the stable final state (midlife) is of interest. A proposed procedure, according to Hasselqvist [18], is as follows:

(1) Perform two load-cycles with virgin material parameters. During these cycles, redistribution of stress and strain occurs in the cyclically loaded structure.
(2) Perform one load-cycle with half-way to midlife material parameters.
(3) Perform one load-cycle with midlife material parameters.
(4) A stabilisation of the cyclic response is assumed, and *e.g.* the fatigue life can be evaluated.

Note that midlife refers to a stable state condition, in which the response is no further changed. One can of course control that a stable cycle has been achieved by comparison to experiments and/or prior knowledge, and if not stable, perform a re-evaluation of the material parameters and re-run the analysis. The evaluated procedure adopted in this study is slightly different from the one described above. The load-cycle at half-way to midlife (point 2) is not performed, as the target is to obtain a stable response at midlife, thus minimising the computational effort. This was both due to that no half-way to midlife cycle was specified in Gustafsson *et al.* [32] and from a speed-up perspective, the half-way to midlife is not of interest. Furthermore, to avoid issues with too rapid changes in the parameters, an incremental transition of the parameters was set up during the load-cycle following the initial two. An accumulative transition which smooths the change during the load-cycle was employed accordingly to

$$x^{n+1} = (1-\theta)x^{n} + \theta\tilde{x} \tag{8}$$

where x are the parameters to be modified in the expressions of the internal variables, which are initially set to the values from Table 1 and incrementally transitioned to the midlife material parameters $\tilde{x}$ with respect to the transition parameter θ. The transition parameter is based on the ratio of the actual time step and the total load-cycle time (peak to peak) with a scale factor, as

$$\theta = \beta\frac{\Delta t}{T_{cycle}} \tag{9}$$

The scale factor β was set to 8 due to that this enable with certainty that the midlife material parameters are obtained prior to the onset of the final load-cycle. During this load-cycle, equilibrium is obtained with respect to the modified parameters, and then a final load-cycle to find the stable midlife response is performed. The local implementation approach was also used here, where the constitutive user-defined material subroutine was updated to modify the material parameters after the two first cycles, according to Equation (8). Hence, the following steps have been applied in this study:

(1) Perform two load-cycles with virgin material parameters. During these cycles, redistribution of stress and strain occurs in the cyclically loaded structure.
(2) Perform one load-cycle where the midlife material parameters are incrementally introduced and find equilibrium.
(3) Perform one load-cycle with the midlife material parameters, where the cyclic response is assumed to be stable.

For the above cycle jumping procedure a new set of material parameters is needed for the midlife cycle. These were obtained by parameter optimisation in which the midlife hysteresis from the experiment was compared to the obtained response from an FE-analysis. The midlife cycle was identified as cycle 300 from the mean stress relaxation behaviour displayed in the paper by Gustafsson *et al.* [32]. The parameters that influence the stress-strain state at midlife are the

Table 2. Material parameters for the midlife cycle.

Parameter	Value	Units
c_1	550.0	GPa
c_2	93.172	GPa
c_3	50.839	GPa
γ_1	2359.802	–
γ_2	680.625	–
γ_3	75.847	–
q_1	− 288.523	MPa
q_2	− 119.991	MPa
q_3	− 240.0	MPa

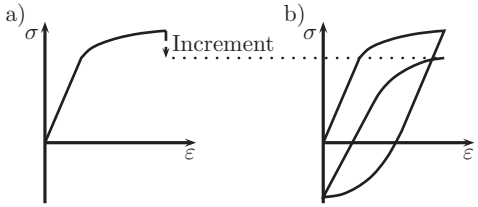

Figure 2. The different approaches to find equilibrium, a) incrementally decreasing the yield stress for a perfect plasticity down-scaled constitutive model or b) perform one load-cycle for a more complex constitutive model.

back-stresses and drag-stresses. For simplicity, the values of the exponents m_k and the rate of softening a_k were kept constant, using the previously defined values. Furthermore, a restriction was placed on q_k to be more negative than the initial values as a lower maximum stress state is present at the midlife cycle compared to the first couple of cycles. The new values describing the midlife cycle are given in Table 2.

A version of the above-presented parameter modification procedure could be to use a down-scaled (less complicated) constitutive model. This saves even more computational effort, and also requires fewer material parameters. Such a constitutive model could, for instance, be defined without a drag-stress term or as a perfect plastic model, and would only require modified back-stress terms or a decrease of the initial yield stress to account for the decrease in mean stress relaxation. To find equilibrium with the latter approach the yield stress needs to be decreased incrementally (successively), as a too large decrease in yield stress would render numerical problems and the algorithm will not likely find $f = 0$, *cf.* Figure 2. This is avoided in the above-presented parameter modification procedure by the inclusion of the load-cycle to find the new equilibrium during which the midlife material parameters are introduced.

Simulation and evaluation

Evaluated component

In order to evaluate the two-cycle jumping procedures, a component with a stress/strain raising feature was to be chosen, as that is the typical critical location for fatigue crack initiation. From this point of view, it is vital that the correct cyclic response is obtained and that the computational time in an industrial context is low, saving development costs and effort. As the component geometry was to have a general relevance, and as it was not to add extra complications or move the focus from the aim of the study, a too detailed or application specific geometry was ruled out. Instead, an unidirectionally loaded plate with a central hole was chosen as the object of study, see Figure 3. Furthermore, a reference simulation was also carried out based on the standard cycle-by-cycle evaluation, for which no cycle jumping procedure was adopted. This reference cycle-by-cycle simulation is used to compare the accuracy of the two evaluated cycle jumping procedures.

The FE-model of the plate was generated only accounting for a quarter of the plate by using symmetry boundary conditions, see Figure 3(b), thus preventing translation in the horizontal direction on the edge between A to B and in the vertical direction on the edge along C to D. The plate is subjected to the cyclic load $\Delta\delta = 0.6\text{mm}$ $(R_\varepsilon = \varepsilon_{min}/\varepsilon_{max} = 0)$. The FE-model consists of a mapped mesh with 228 fully integrated 8-noded brick elements (one element through the thickness) and was analysed in the FE-software LS-DYNA [40], version R7, using an implicit solution technique coupled with the three implemented user-defined material subroutines (one for each solution approach). The response in the highly loaded element in the top of the hole (at B) was extracted during the entire loading sequence. The response at this point will be the most damaging to the structure from a fatigue point-of-view, as cyclic loading produces considerable plastic deformation which for a real application

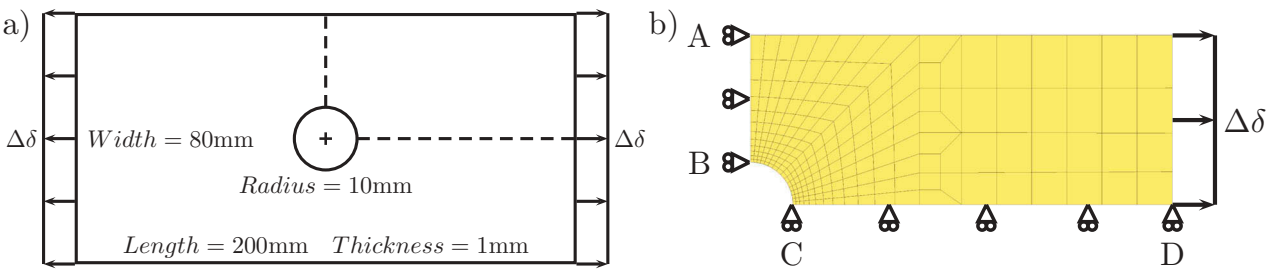

Figure 3. The a) evaluated plate with the centred hole, and the used b) FE-model with symmetry boundary conditions.

Table 3. The CPU time for each simulation.

Simulation	CPU time	Relative time
Reference	89h 56min 49s	56.02
Extrapolation	25h 33min 32s	15.92
Modification	1h 36min 20s	1

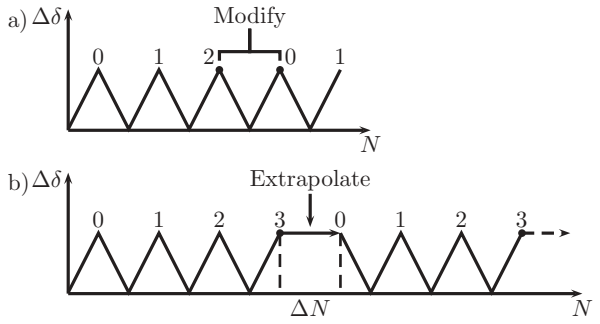

Figure 4. Loading sequence for a) parameter modification and b) extrapolation.

eventually might lead to crack initiation and subsequent crack growth. Thus, it is of high importance that a correct response is obtained in locations like this when designing gas turbine components subjected to cyclic loading conditions.

The FE-simulations were performed on a Linux-based cluster, equipped with four Intel(R) Xeon(R) CPU E5 − 2650 v2 @ 2.60GHz eight-core processors. Eight cores were used in each simulation, giving equal conditions for the comparison. The consumed computational time (CPU time) for each of the three different simulations can be found in Table 3.

Loading sequence

The loading sequence is different for the two investigated cycle jumping procedures, see Figure 4. For the material parameter modification procedure, the loading is conveyed by a sequence of 4.5 cycles, in which the first on-loading (0.5 cycle, defined as cycle 0) is not included in the evaluation due to initial plasticity and redistribution of the stress state. After two unloading-loading cycles (1 − 2), the set of the modified material parameters based on the midlife properties are incrementally introduced during the full new initial cycle (0) to find equilibrium. Finally, a last cycle is performed to obtain a stable hysteresis loop with the modified parameters.

When it comes to the extrapolation procedure, only two consecutive cycles could have been performed, but due to numerical stability, three consecutive cycles (1 − 2 − 3) were used. Furthermore, the initial on-loading (0) is not included here either, for the same reasons as discussed above. Then, an extrapolation step is performed generating new values of the variables in the response set, in which the load is kept constant to yield equilibrium at the new initial step (0). The above-described loading sequence is then repeated until the stabilised state at midlife is obtained. In the case of the local implementation approach, no stability condition can be present, as no global stability can be determined, and thus the analysis was terminated at $N = 300$ (midlife). Lastly, the reference cycle-by-cycle simulation was performed with continuous loading and unloading until 300 cycles were reached. The same amount of cycles were evaluated in all cases for comparative reasons.

Results and discussion

From the simulations, it can be seen that a cycle jumping procedure will lower the computational effort profoundly, see Table 3. Depending on which type of cycle jumping procedure that is used, different levels of efficiency are obtained. As can be seen in Figure 5, the good accuracy of the different simulation methods is noteworthy. However, the extrapolation method does not exactly predict the same increasing maximum and minimum stress levels after about 50 cycles compared to the reference simulation, see Figure 5(c–d). A reason can be the larger extrapolation steps compared to during the first four cycle jumps that increases the uncertainties with the extrapolation method. A second-order extrapolation approach or an adaptive extrapolation stepping approach with convergence criterion might generate better resolution of the predictions, but from a global perspective, a good agreement is achieved with this simple extrapolation method, *cf.* Figure 5(a). Moreover, the parameter modification cycle jumping procedure generates a midlife response that is in-line with both the extrapolation method and the reference 'cycle-by-cycle' simulation. A small shift 'upwards' can be noticed at midlife, but it is only by a few MPas, *cf.* Figure 5. Further, the large compressive state seen in Figure 5(d) for the modification method is the reversed loading peak in the cycle prior to midlife. This peak is not to be mistaken for the midlife response, as during this cycle the new set of material parameters are introduced and equilibrium is acquired. The good response is further enhanced when comparing the hysteresis loops at the midlife cycle of the different simulations, see Figure 6. One can note that the shape of the hysteresis loops differs. This is due to that the new parameters in the modification procedure has been obtained based on the actual midlife hysteresis from the experiment in Gustafsson *et al.* [32], and the two other methods are dependent on the constitutive model to generate the hysteresis loops based on evolution with the initially defined parameters. Hence, a discrepancy is obtained due to the accurateness of the constitutive model, and it is likely that a small deviation will always be present as the reference and extrapolation models will not precisely predict the midlife cycle as good as the new set of parameters used in the parameter modification

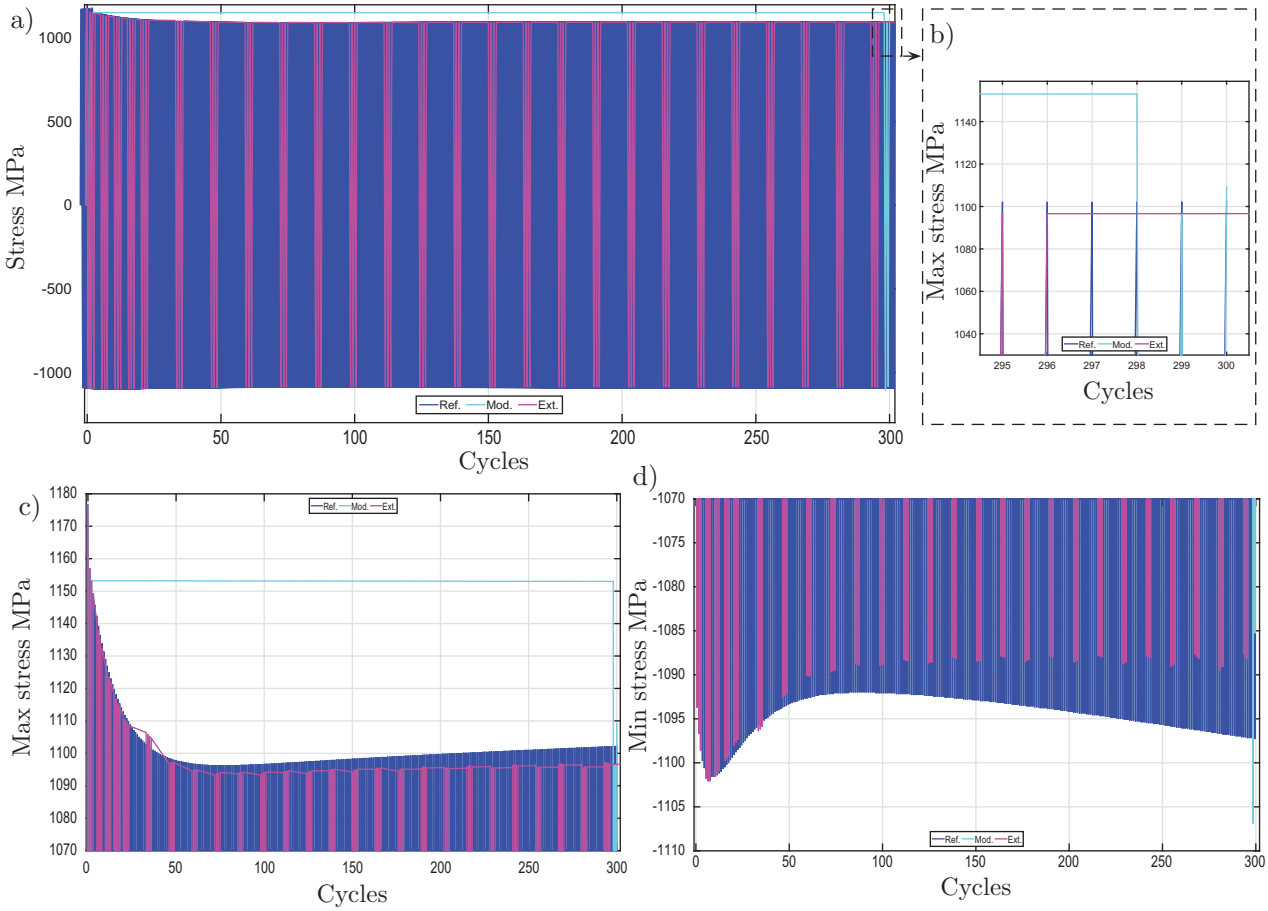

Figure 5. Stress versus cycle response from the three FE-simulations, displaying a) the entire stress history, b) the maximum stress at midlife, c) the maximum stress and d) the minimum stress evolution.

method does. In addition, the difference can also be due to that a different approach might have been employed when calibrating the midlife material parameters compared to the initial material parameters defined in Gustafsson *et al.* [32]. These might be reasons for the slightly different response at the midlife cycle. Furthermore, all data points were not explicitly available and a puzzling operation had to be performed to acquire the material response from the experiments. This could, of course, generate errors in the material parameters, which might be further accentuated in the FE-simulation. Another, close-related issue is the choice of the adopted constitutive model and the ongoing amount of back-stress and drag-stress terms. The model has been chosen based on industrial relevance, and the number of terms gives a good representation of the material behaviour. Of course, one could have used more terms to enhance the correlation to the observed material behaviour or less to minimise the calibration process (practical for the parameter modification method). It can also be seen in Figure 6 that the strain range of the hysteresis loops does not match between the different simulations, especially the extrapolation method. This can be due to that the accumulated plastic strain locally in the element of interest (at B in Figure 3(b)) is different, and that the element becomes more severely deformed with each cycle. The more performed cycles generate a larger plastic strain range in subsequent hysteresis loops. Moreover, the horizontal and inclined lines for the modification and extrapolation method in Figure 5, are purely graphical. The stress states during these time intervals are not generated in the material model, but they give an estimate of the increase or decrease of the stress state between the skipped cycles, especially for the extrapolation method. In the case of the modification method, the stress state is kept constant during the skipped cycles, and then one load-cycle is performed with the introduction of the new material parameters to acquire equilibrium, cf. Figure 2, thus the horizontal line.

The ability to speed-up the computational time is of essence, as one load-cycle takes approximately 18min, implying that every cycle counts. From the performed simulations, the parameter modification cycle jumping procedure is the fastest one, see Table 3. The computation time is reduced by a factor of 15.92 compared to the extrapolation method and 56.02 compared to the reference cycle-by-cycle simulation. Though, one needs to keep in mind that no evolution of the internal variables is updated within the modification method, and thus one lack knowledge about *e.g.* the continuous

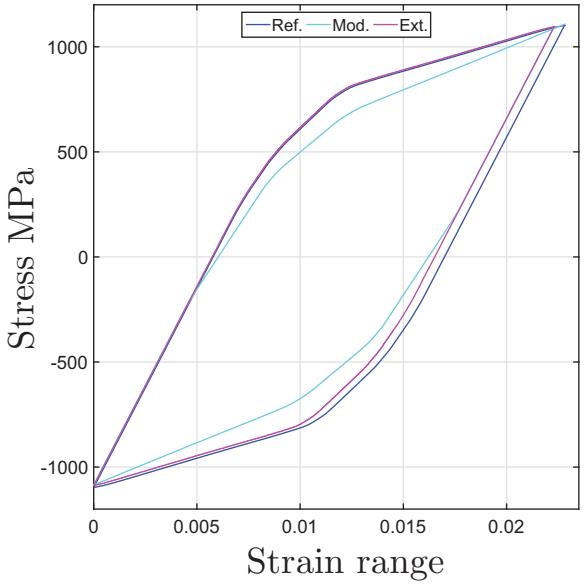

Figure 6. Hysteresis loops at the midlife cycle.

'cycle-by-cycle' damage accumulation to be used in, for instance, a fatigue evaluation. Moreover, it is also to be mentioned that a fatigue evaluation is often performed by evaluating the obtained hysteresis loop with respect to *e.g.* a Coffin-Manson type of expression, and this is easily done with the modification method at the stable midlife cycle. Furthermore, it is stressed that these responses are a result of the specific load-case and current cycle jumping procedures. With this specified, the pros and cons of the two cycle jumping methods are given in Table 4.

To speed-up the extrapolation procedure a dynamic ΔN could be used, as discussed earlier regarding the local and global implementation approach. A dynamic extrapolation procedure was investigated where ΔN was increased at discrete times, but due to a stability problem this approach was not further investigated and a static step was used throughout the simulation (except for the first four extrapolation steps). The reason for the stability issue refers to a too large extrapolation step in the area where the maximum stress starts to increase during the loading sequence. It can be observed in Figure 7 that the discrepancy between the extrapolated state and following stabilising cycle becomes large at specific times (steep slope), which will be further enhanced by a large extrapolation step. This can result in a response that the non-linear solver is not able to handle. An adaptive extrapolation stepping functionality might render a solution for this problem using a global implementation approach. In addition, it is further stressed that no intention was to develop a robust dynamic approach, where the steps could be changed as a function of the response or the time, or an as good as possible extrapolation jumping scheme. The aim is just to compare with the modification method. Of course, there are many innovative approaches that handle the continuous accuracy, stability and speed-up process in a far more better way, see *e.g.* [10] or [2]. It is also to be mentioned, that as the parameter modification method generates no history evolution; consequently, no stress evolution is present as can be seen in Figure 7, also *cf.* Figure 5(c) . Hence, the observed drift in stress for the reference and extrapolation simulations can never be obtained with the parameter modification-jumping procedure, as it is a discrete method evaluating the behaviour at the specific midlife cycle where the constitutive parameters have been evaluated.

Table 4. Pros and cons for the two different cycle jumping procedures.

Method	Pros	Cons
Modification	+ Very fast, only 4.5 cycles	– No evolution history
	+ Simple	– Evaluation of two material parameter sets
	+ Stable	
Extrapolation	+ Evolution history	– Static extrapolation step (local) = slow
	+ One material parameter set	– Complex implementation (global)
	+ Access to any hysteresis loop	– May give stability issues for large extrapolation steps

The local implementation approach saves computational time in the extrapolation cycle jumping procedure with respect to a global approach. This is due to that the FE-simulation do not have to be restarted and all internal variables do not have to be mapped on the mesh for each cycle. But in the local implementation approach, it will be difficult to have a global termination criterion in which the stability is monitored, as the neighbouring element might generate a stress state that does not meet the control criteria, and the one you are analysing might do so. Hence, a contradiction has arisen, and the criteria is not generally applicable for the entire FE-model. This is a lot easier in a global approach with a tolerance measure, as the extrapolation procedure is executed after a completed time-step in the FE-analysis instead of during the time-step, where an accuracy control and termination criterion can, for instance, be based on the global stress state, *cf.* Figure 8. However, in Figure 7 it can be seen that the global maximum stress is slowly increasing with each cycle after, approximately, the 85th cycle. Hence, such a global termination criteria might generate unwanted consequences, and thus one needs to account for the small increase in a potential termination criterion of such character or base the criterion on some other entity.

As one of the main driving forces to speed-up, the computational effort is related to fatigue, and prediction of the fatigue life of an industrial component, the choice of fatigue identification parameter is highly dependent on the chosen cycle jumping method. For the extrapolation procedure, all the history is

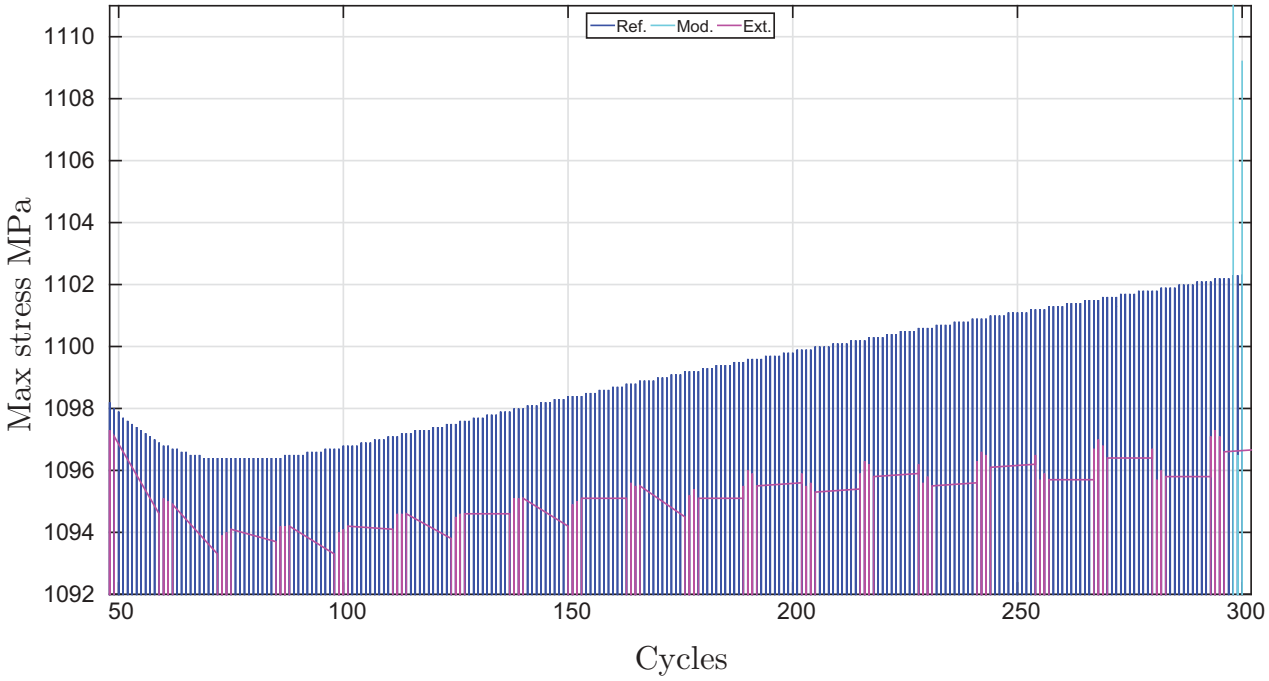

Figure 7. The maximum stress versus cycles for the different simulations.

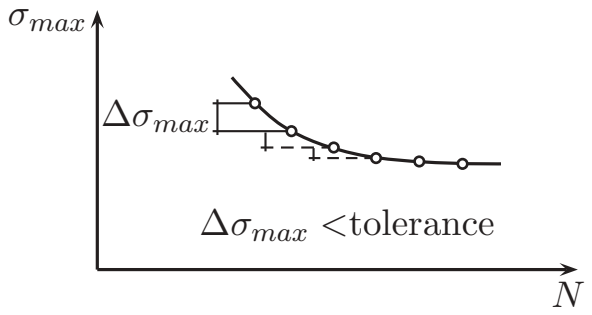

Figure 8. Tolerance measure with respect to the global maximum stress from each cycle as the termination criterion.

present and the definition of the fatigue parameter can be chosen relatively freely (depending on the application). A traditional post-processing, extracting amplitudes, ranges or max and min values, *cf.* Ince and Glinka [41], can be adopted as well as a continuously accumulated fatigue damage parameter over the cycles, see *e.g.* Leidermark *et al.* [42]. In the case of the parameter modification procedure, a cyclic accumulative approach is not an option, as the intermediate cycles have been skipped. Secondly, the type of adopted constitutive model at the jumped state is of great importance. Here, a down-scaled material model, *e.g.* perfect plastic or linear kinematic behaviour, will not generate the accurate non-linear shape of the hysteresis. Hence, if a dissipative energy criterion is considered as fatigue identification parameter, *cf.* Cruzado *et al.* [43], then differences compared to a complex non-linear material description will be present in the fatigue life predictions. On the other hand, a fatigue identification parameter dependent on, for instance, ranges can still be adopted in this case.

An important aspect from a design perspective is that a highly accurate response might not necessarily be the target. It might be that only a fast response is needed to get a first picture of the stress/strain state, and from this, the design may be changed and re-evaluated. This promotes the parameter modification procedure over the extrapolation method, even though one has to evaluate two sets of material parameters which is time-consuming. On the other hand, one does not necessarily have to perform all the extrapolation steps to acquire a response that is suitable to use in an evaluation. Instead, one can, as discussed above, settle for a response that gives a satisfying response during the design process to get a first estimate. To sum it up, use the fast discrete parameter modification method iteratively in the early stages of the design process. Then, perform more accurate calculations at the end of the process using the full extrapolation method accounting for various stability conditions, accuracy controls and termination criteria.

Conclusions

Based on the above-presented cycle jumping study for a simple component, with a relevant disc alloy material description, the following conclusions may be drawn:

(a) A large difference in computational time between the three simulation approaches can be observed. The more cycles computed the

more effort is needed. Here, the discrete parameter modification cycle jumping procedure is with margin the fastest one.

(b) The parameter modification cycle jumping procedure is very simple and stable, but one needs to evaluate two sets of material parameters, which can be hard and, in itself, time-consuming. However, a down-scaled constitutive model can be used for the midlife cycle with fewer material parameters, reducing this effort.

(c) In the extrapolation cycle jumping procedure the evolution history is obtained, but it may be unstable for large extrapolation step sizes. An adaptive extrapolation stepping functionality with a global implementation approach might be a way to solve this.

(d) The local implementation approach gives direct control of the cycle jumping procedure, and no mapping of the variables in the response set or restarts of the FE-analysis need to be performed. However, a global implementation approach can be used to enable control over the accuracy, stability conditions and termination criterion of the cycle jumping procedure with respect to *e.g.* the global stress state.

(e) During the initial design process, the parameter modification method offers fast and reliable results for a first estimate by using minimal resources.

Acknowledgments

The study has received funding from the Clean Sky 2 Joint Undertaking under the European Union's Horizon 2020 research and innovation programme under grant agreement No 686600.

Disclosure statement

No potential conflict of interest was reported by the authors.

Funding

This work was supported by the Cleansky [686600]; Cleansky [686600];

References

[1] Nesnas K, Saanouni K. A cycle jumping scheme for numerical integration of coupled damage and visco-plastic models for cyclic loading paths. Revue Européenne Des Éléments Finis. 2000;9:865–891.

[2] Cojocaru D, Karlsson AM. A simple numerical method of cycle jumps for cyclically loaded structures. Int J Fatigue. 2006;28:1677–1689.

[3] Bogard F, Lestriez P, Guo YQ. Damage and rupture simulation for mechanical parts under cyclic loadings. J Eng Mater Technol. 2010;132:021003.

[4] Brommesson R, Ekh M. Modelling of cyclic behaviour of haynes 282 at elevated temperatures. Mater High Temp. 2014;31:121–130.

[5] Diel S, Huber O. A continuum damage mechanics model for the static and cyclic fatigue of cellular composites. Materials. 2017;10:951–972.

[6] Kindrachuk VM, Unger JF. A fourier transformation-based temporal integration scheme for viscoplastic solids subjected to fatigue deterioration. Int J Fatigue. 2017;100:215–228.

[7] Zhang Y, Lu L, Gong Y, Zhang JZeng D. Finite element modeling and experimental validation of fretting wear scars in a press-fitted shaft with an open. Zone,tribology Transactions. 2018;61:585-595. DOI: 10.1080/10402004.2017.1378395

[8] Shojaei AK, Wedgewood AR. An anisotropic cyclic plasticity, creep and fatigue predictive tool for unfilled polymers. Mech Mater. 2017;106:20–34.

[9] Rezazadeh M, Carvelli V. A damage model for high-cycle fatigue behavior of bond between frp bar and concrete. Int J Fatigue. 2018;111:101–111.

[10] Lin J, Dunne FPE, Hayhurst DR. Approximate method for the analysis of components undergoing ratchetting and failure. J Strain Anal. 1998;33:55–64.

[11] Johansson G, Ekh M. On the modeling of large ratcheting strains with large time increment. Int J Comput-Aided Eng Soft. 2007;24:221–236.

[12] Bogard F, Lestriez P, Guo YQ. Numerical modeling of fatigue damage and fissure propagation under cyclic loadings. Int J Damage Mech. 2008;17:173–187.

[13] Burlon S, Mroueh H, Cao JP. 'skipped cycles' method for studying cyclic loading and soil-structure interface. Comput Geotech. 2014;61:209–220.

[14] Wang P, Cui L, Lyschik M, et al. A local extrapolation based calculation reduction method for the application of constitutive material models for creep fatigue assessment. Int J Fatigue. 2012;44:253–259.

[15] Kontermann C, Scholz A, Oechsner M. A method to reduce calculation time for fe simulations using constitutive material models. Mater High Temp. 2014;31:334–342.

[16] Abaqus, abaqus 6.12 documentation, dassault systèmes, providence, usa; 2014.

[17] Brommesson R, Ekh M, Hörnqvist M. Correlation between crack length and load drop for low-cycle fatigue crack growth in ti-6242. Int J Fatigue. 2015;81:1–9.

[18] Hasselqvist M Aspects of creep-fatigue in gas turbine hot parts [dissertation]. Linköping University; 2001.

[19] Hyde CJ, Sun W, Hyde TH, et al. Thermo-mechanical fatigue testing and simulation using a viscoplasticity model for a p91 steel. Comput Mater Sci. 2012;56:29–33.

[20] Moverare JJ, Kontis P, Johansson S, et al. Thermomechanical fatigue crack growth in a cast polycrystalline superalloy. MATEC Web of Conferences. 2014;14:19004.

[21] Maier G, Hübsch O, Somsen C, et al. Cyclic plasticity and lifetime of the nickel-based alloy c-263: experiments, models and component simulation. MATEC Web of Conferences. 2014;14:16006.
[22] Pang HT, Reed PAS. Microstructure effects on high temperature fatigue crack initiation and short crack growth in turbine disc nickel-base superalloy udimet 720li. Mater Sci Eng A. 2007;448:67–79.
[23] Zhu SP, Huang HZ, He LP, et al. A generalized energy-based fatigue-creep damage parameter for life prediction of turbine disk alloys. Eng Fract Mech. 2012;90:89–100.
[24] Sudarshan Rao G, Sharma VMJ, Thomas Tharian K, et al. Study of lcf behavior of in718 superalloy at room temperature. Mater Sci Forum. 2012;710:445–450.
[25] Musinski WD, McDowell DL. Microstructure-sensitive probabilistic modeling of hcf crack initiation and early crack growth in ni-base superalloy in100 notched components. Int J Fatigue. 2012;37:41–53.
[26] Dong K, Yuan C, Gao S, et al. Creep properties of a powder metallurgy disk superalloy at 700°c. J Mater Res. 2017;32:624–633.
[27] Ahmed R, Barrett PR, Hassan T. Unified viscoplasticity modeling for isothermal low-cycle fatigue and fatigue-creep stress-strain responses of haynes 230. Int J Solids Struct. 2016;88–89:131–145.
[28] Saxena A. Creep and creep-fatigue crack growth. Int J Fract. 2015;191:31–51.
[29] Lundström E, Simonsson K, Gustafsson D, et al. A load history dependent model for fatigue crack propagation in inconel 718 under hold time conditions. Eng Fract Mech. 2014;118:17–30.
[30] Wilcock IM, Cole DG, Brooks JW, et al. Elevated temperature cyclic stress-strain behaviour in nickel based superalloys. Mater High Temp. 2002;19:187–192.
[31] Yu H, Li Y, Huang X, et al. Low cycle fatigue behavior and life evaluation of a p/m nickel base superalloy under different dwell conditions. Procedia Eng. 2010;2:2103–2110.
[32] Gustafsson D, Moverare JJ, Simonsson K, et al. Modeling of the constitutive behavior of inconel 718 at itermediate temperatures. J Eng Gas Turbine Power. 2011;133:094501.
[33] Prasad K, Sarkar R, Ghosal P, et al. High temperature low cycle fatigue deformation behaviour of forged in 718 superalloy turbine disc. Mater Sci Eng A. 2013;568:239–245.
[34] Cruzado A, Llorca J, Segurado J. Modeling cyclic deformation of inconel 718 superalloy by means of crystal plasticity and computational homogenization. Int J Solids Struct. 2017;122–123:148–161.
[35] Ohno N, Wang JD. Kinematic hardening rules with critical state of dynamic recovery, part i: formulation and basic features for ratchetting behavior. Int J Plast. 1993;9:375–390.
[36] Ohno N, Wang JD. Kinematic hardening rules with critical state of dynamic recovery, part ii: application to experiments of ratchetting behavior. Int J Plast. 1993;9:391–403.
[37] Chaboche JL. A review of some plasticity and viscoplasticity constitutive theories. Int J Plast. 2008;24:1642–1693.
[38] Chaboche JL. Constitutive equations for cyclic plasticity and cyclic viscoplasticity. Int J Plast. 1989;5:247–302.
[39] Matlab r2015a. The mathworks Inc., Natick; 2018.
[40] Hallquist JO. Ls-dyna theory manual. Livermore: Livermore Software Technology Corporation; 2006.
[41] Ince G, Glinka G. A generalized fatigue damage parameter for multiaxial fatigue life prediction under proportional and non-proportional loadings. Int J Fatigue. 2014;62:34–41.
[42] Leidermark D, Eriksson R, Rouse JP, et al. Thermomechanical fatigue crack initiation in disc alloys using a damage approach. MATEC Web Conf, 12th International Fatigue Congress. 2018;165:19007.
[43] Cruzado A, Lucarini S, Llorca J, et al. Microstructure-based fatigue life model of metallic alloys with bilinear coffin-manson behavior. Int J Fatigue. 2018;107:40–48.